
Hiroshima University Institutional Repository

Role of cell proliferation in strobilation of moon jellyfish *Aurelia coerulea*

Karin Fujii[1*], Hiroki Koyama[2] and Hisato Kuniyoshi[1, 3]

[1]Program of Food and AgriLife Science, Graduate School of Integrated Sciences for Life, Hiroshima University, Higashi-hiroshima 739-8528, Japan

[2]Department of Food Science and Technology, Tokyo University of Marine Science and Technology, Tokyo 108-8477, Japan

[3]Seto Inland Sea Carbon-neutral Research Center, Hiroshima University, Higashi-hiroshima 739-8528, Japan

***Corresponding author:**

Karin Fujii

E-mail; karinfujii@hiroshima-u.ac.jp, Tel; +81-82-424-7948, Fax; +81-82-424-2459

Hiroki Koyama

E-mail; hkoyam1@kaiyodai.ac.jp

Hisato Kuniyoshi

E-mail; hkuni@hiroshima-u.ac.jp

Abstract

The life cycle of the moon jellyfish *Aurelia coerulea* is composed of sessile polyp and free-swimming jellyfish stages. Strobilation is a polyp-to-jellyfish transition comprising sequential segment formation (segmentation), subsequent morphogenesis into ephyrae (young jellyfish), and detachment of the ephyrae. Cell proliferation is involved in metamorphosis in various animals. In the present study, we examined the relationship between cell proliferation and strobilation in *A. coerulea*. To visualize cell proliferation at various stages of strobilation, 5-bromo-2'-deoxyuridine labeling experiments were conducted, in which cell proliferation was distributed in the segments and prospective regions of the next segment during segmentation. Cell proliferation in segments continues during ephyra morphogenesis. Hydroxyurea, a cell-cycle inhibitor, was administered to investigate cell proliferation in animals at different stages of strobilation. In this study, hydroxyurea interrupted the initiation of strobilation, segmentation, and ephyra morphogenesis, but not ephyra detachment. This suggests that cell proliferation plays a crucial role in generating a new segment and constructing the ephyra body.

Keywords: *Aurelia coerulea*; cell proliferation; jellyfish; polyp; strobilation

Introduction

Cnidaria is a large animal phylum that includes two major groups: Medusozoa (Staurozoa, Cubozoa, Scyphozoa, and Hydrozoa) (jellyfish and hydra) and Anthozoa (corals and sea anemones) (Collins et al. 2006). Many Cubozoa, Scyphozoa, and Hydrozoa species have a complex life cycle comprising benthic polyp and planktonic jellyfish stages. One example is the life cycle of the moon jellyfish *Aurelia coerulea* (Scorrano et al. 2016, previously described as *Aurelia* sp. 1 by Dawson and Jacobs 2001). Fertilized *A. coerulea* eggs develop into swimming planular larvae, which then metamorphose into sessile polyps after settling on a substrate. Polyps propagate asexually by fission and budding. In response to environmental stimuli such as decreased water temperature, polyps turn into strobilae that possess multiple transverse segments on their body column. Each segment metamorphoses into an ephyra. Eventually, several ephyrae are released from a single strobila (Fig. 1). This polyp-to-jellyfish transition in *Aurelia* is known as strobilation.

Aurelia strobilation is comprised of four temporal stages: initiation of strobilation, segmentation, ephyra morphogenesis, and ephyra detachment. Initiation of strobilation can be induced by indole compounds, such as indomethacin (Kuniyoshi et al. 2012) and 5-methoxy-2-methylindole (Fuchs et al. 2014; Helm and Dunn 2017). Fuchs et al. (2014) reported that 9-*cis* retinoic acid and WSRRRWL heptapeptide may be endogenous strobilation-initiating factors. In segmentation, a constriction forms beneath the tentacles, and additional constrictions are generated sequentially from oral to aboral. The region between two constrictions corresponds to a segment. In the case of *Aurelia*, the number of segments varies, and larger polyp sizes tend to produce a greater number of segments (Kroiher et al. 2000). Kraus et al. (2015) reported an evolutionary developmental study of ephyra morphogenesis, during which each segment develops into an ephyra. We have also revealed that lysosomal hydrolases are related to ephyra morphogenesis in the oral end segment (Tsujita et al. 2017).

Cell proliferation plays an important role in the metamorphosis of various animals. In the African-clawed frog, *Xenopus laevis*, cell proliferation has been observed only in the adult epithelia of the intestines in the larval epithelia during metamorphosis (Ishizuya-Oka and Ueda 1996). In the fruit fly *Drosophila melanogaster*, cell proliferation in wing discs is involved in wing morphogenesis during the pupal stage (Milan et al. 1996). Cell proliferation is involved in cnidarian metamorphosis. In the Cubozoan species *Tripedalia cystophora* and *Alatina moseri*, cell proliferation occurs in regions where rhopalia (sensory structures), jellyfish tentacles, manubria, and gastric filaments are generated during polyp-to-

jellyfish metamorphosis (Gurska and Garm 2014). In the hydrozoan jellyfish *Cladonema pacificum*, it was detected in the umbrellas and tentacles of young jellyfish during the appendage morphogenesis (Fujita et al. 2019). In *Hydractinia echinata* (Hydrozoa), cell proliferation has been observed in the gastric region during metamorphosis from planulae to primary polyps (Plickert et al. 1988). In *Aurelia* (Scyphozoa), during planula-to-polyp metamorphosis, cell proliferation was observed in the oral region of the planulae, particularly in the earlier stages, and in the more aboral region in the later stages (Gold et al. 2016). Based on Balcer and Black (1991), cell proliferation was detected using ^{3}H-labeled thymidine incorporation during *Aurelia* strobilation, and hydroxyurea (HU), a cell cycle inhibitor, interrupted strobilation. However, the stage-associated roles of cell proliferation remain poorly understood, as the strobilation stages are yet to be clearly defined.

In the present study, the role of cell proliferation, focusing on the temporal stages of strobilation, was investigated by characterizing the external and internal morphologies of the polyp/strobila at each stage. Cell proliferation patterns at every stage of strobilation were examined using 5-bromo-2'-deoxyuridine (BrdU) labeling. The requirements of cell proliferation at each stage of strobilation were verified by administering HU and the defects caused by HU were histologically analyzed.

Materials and methods

Animals

All the experiments were performed using clonal polyp strains of *A. coerulea* from the Seto Inland Sea, Japan. Polyps were cultured in filtered seawater (FSW) at 23 ºC. The polyps were fed twice weekly with newly hatched *Artemia* and water was replaced 3–5 h after feeding. Animals were starved for more than 1 week prior to the experiments. A stereomicroscope (Stemi 305 CAM) with an integrated camera (ZEISS, Jena, Germany) was used to observe the animal morphology.

Strobilation was induced by decreasing the water temperature from 23 ºC to 10 ºC (cold shock; CS) (Kuniyoshi et al. 2012; Kroiher et al. 2000) or by the administration of 5-methoxy-2-methylindole (MMI) (Fuchs et al. 2014). In this study, the following terminology is used: The onset of strobilation was defined as the appearance of the first constriction beneath the tentacles (Fig. 1c). The CS- or MMI-treated animal before the onset of strobilation, which had not yet shown any morphological change, was termed "prestrobila" (Fig. 1b). Initiation of strobilation means the period from the prestrobila to the onset of

strobilation. The earlier phase of strobilation, in which segments were generated sequentially from the oral side to the aboral side, was named the "segmentation phase" (Fig. 1c–e). The later phase of strobilation, in which each segment developed into an ephyra, was called the "ephyra morphogenesis phase" (Fig. 1f–h). The last phase of strobilation, in which each segment was liberated as an ephyra, was called the "ephyra detachment phase" (Fig. 1i). The end of strobilation was defined as the detachment of all ephyrae. A segment refers to the region between the oral end and the first constriction or the region between two constrictions (Tsujita et al. 2017) so that the number of segments in a strobila is equivalent to the number of ephyrae released from the strobila.

Preparation of paraffin sections

Polyps and strobilae were anesthetized in 0.17 M $MgCl_2$ (1 M $MgCl_2$:FSW = 1:5) for five min. The animals were fixed with 4% formaldehyde in artificial seawater (ASW) (Nihonkaisui, Tokyo, Japan) for 1 h at room temperature and then washed with ASW for 30 min on ice. The fixed animals were dehydrated in an ethanol series (25%, 50%, 75%, 80% ethanol/ASW; 80%, 90%, 95% ethanol/water; and ethanol). Following incubation with xylene at room temperature, the samples were embedded in paraffin blocks, cut into 5-µm-thick sections with a microtome blade (A35, FEATHER, Osaka, Japan) on a rotary microtome (RM2125RTS, LEICA, Nussloch, Germany), and placed onto MAS adhesive glass slides (MATSUNAMI, Osaka, Japan).

Hematoxylin-eosin (HE) stain

The sections were deparaffinized with xylene and then rehydrated in an ethanol series (100%, 90%, 80%, and 70% ethanol/water). Following a five-min wash in water, the sections were stained with eosin Y (MUTO PURE CHEMICALS, Tokyo, Japan) and Mayer’s hematoxylin. After the sections were dehydrated in ethanol, followed by xylene, coverslips were mounted onto slides using Multi Mount 480 (MATSUNAMI). Sections were observed under an ALPHAPHOT YS optical microscope (Nikon, Tokyo, Japan) equipped with a camera (3R-DMKC01, 3R SOLUTION; Fukuoka, Japan).

BrdU labeling experiment

Polyps were collected from a Petri dish that was cultured at 23 ºC. The CS-treated prestrobilae and segmentation-phase strobilae were collected from a Petri dish that was cultured at 10 ºC for 38–50

days, and ephyra-morphogenesis-phase strobilae were collected from a Petri dish that was cultured at 10 ºC for 64 days. Collected animals were incubated in FSW containing 10 mM BrdU (Cayman Chemical, MI, USA) at 23 ºC for 48 h for the polyps and 24 h for the prestrobilae and strobilae, followed by fixation with 4% formaldehyde in ASW (Fig. 3). Paraffin-embedded sections were prepared as previously described. Sections were deparaffinized with xylene and then rehydrated in an ethanol series (100%, 90%, and 80% ethanol/water). All the incubations were performed at room temperature. Following three washes in phosphate buffered saline plus Triton-X (PBST; 10 mM phosphate buffer [pH 7.5], 0.15 M NaCl, 0.1% [v/v] Triton-X 100), the sections were treated with 2 M HCl for 10 min, rinsed with PBST three times, and then preincubated with a blocking solution (1% [w/v] bovine serum albumin [Sigma-Aldrich, MO, USA], and 2% [v/v] normal sheep serum [CHEMICON, CA, USA], PBST) for 30 min. To detect BrdU incorporation in the nuclei, the sections were incubated with a rabbit anti-BrdU polyclonal antibody (GeneTex, CA, USA) diluted 1:500 with blocking solution for 3 h. After three washes in PBST, the sections were incubated for 1 h with an alkaline phosphatase-conjugated anti-rabbit IgG antibody (Sigma-Aldrich) diluted 1:1000 in the blocking solution. After three washes in PBST, the sections were incubated in 1 M Tris-HCl (pH 9.5) containing 2 mM levamisole hydrochloride (Nacalai Tesque, Kyoto, Japan) to inhibit endogenous alkaline phosphatase activity. Signals were visualized by incubating the sections with a substrate solution (125 µg/mL BCIP [5-bromo-4-chloro-3-indolyl phosphate *p*-toluidine salt; Nacalai Tesque], 250 µg/mL NBT [nitro blue tetrazolium; Nacalai Tesque], 1 mM levamisole hydrochloride, and 1 M Tris-HCl [pH 9.5]) for 15–20 min. The sections were rinsed with water to stop the reaction and then dehydrated in ethanol followed by xylene. Coverslips were mounted onto slides using a Multi Mount 480 (MATSUNAMI) and observed with an ALPHAPHOT YS microscope (Nikon) equipped with a camera (3R-DMKC01, 3R SOLUTION).

Administration of the cell cycle inhibitor, HU

A single polyp was placed in the well of a 24-well microtiter plate and incubated in 1 mL FSW containing 10 nM MMI (Alfa Aesar, Lancashire, United Kingdom) at 23 ºC. The administration schedule of HU (FUJIFILM Wako Pure Chemical Corporation, Osaka, Japan) is shown in Fig. 5. In experiment A, 10 mM HU was co-administered with MMI. In experiments B, C, and D, HU was added 24, 48, and 72 h after the administration of MMI, respectively. HU was not added to the control group. The morphology of each tested animal was observed for 10 days using a stereomicroscope (Stemi 305 cam) with an integrated

camera (ZEISS). The number of segments was recorded daily over a 10-day observation period. The increase in the number of segments (Δsegment) after HU administration in experiment C was calculated as follows:

$$\Delta segment = (number\ of\ segments\ at\ 10\ days\ after\ MMI\ administration) - (number\ of\ segments\ at\ 48\ h\ after\ MMI\ administration)$$

The number of segments and Δsegment values of experimental animals were statistically compared with those in the control using the Mann–Whitney *U* test with Bonferroni correction.

Results

Morphological observations of strobilation

Based on the observations of the changes in external morphology during strobilation, it was found that the CS-treated polyps showed minimal changes for over a month (Fig. 1b; prestrobila). The first constriction appeared beneath the tentacles 5–8 weeks after CS (Fig. 1c; defined as the onset of strobilation). Additional segments were sequentially generated toward the aboral side (Fig. 1d, e; segmentation phase). The segmentation phase continued for approximately 2 weeks. Upon becoming fully segmented strobilae, the tentacles around the mouth degenerated in approximately 2 days (Fig. 1f; early ephyra morphogenesis phase). After tentacle degeneration, each segment developed ephyra morphology in approximately 1 week (Fig. 1g; middle ephyra morphogenesis phase) and then started pulsating (Fig. 1h; late ephyra morphogenesis phase). After ephyra morphogenesis, the ephyrae were sequentially released in an oral-to-aboral direction (Fig. 1i; ephyra detachment phase). All ephyrae (Fig. 1j) were detached in approximately 1 week with the foot region left behind. This residual foot region, called the residuum (Fig. 1k), was similar in morphology to the polyp morphology (Fig. 1a). Eventually, the same number of ephyrae as segments were released from one polyp.

HE staining of paraffin-embedded sections showed that the whole body of the polyps exhibited a sac-like structure composed of two cell layers: the ectoderm and endoderm (Fig. 2a, f).

Longitudinal sections of the prestrobilae also showed a sac-like body with two epithelial cell layers (Fig. 2b, g), similar to those of the polyps (Fig. 2a, f). Thus, no difference in internal morphology

was found between the polyps and prestrobilae.

In the longitudinal sections of the segmentation-phase strobilae, both the endodermal and ectodermal epithelial cell layers repetitively invaginated into the gastric cavity to produce segments (Fig. 2c, h). The tips of the invaginations were unfused at the constrictions, and the gastric cavity remained continuous from the mouth to foot region. Consequently, the gastric cavity exhibited accordion-like folding.

Invaginations of the two epithelial cell layers were deeper in the longitudinal sections of the middle ephyra-morphogenesis-phase strobilae (Fig. 2d, i) than in those of the segmentation-phase strobilae (Fig. 2c, h). Similarly, the tips of the invaginations were not fused at the constrictions. Hence, the ephyra-morphogenesis-phase strobilae maintained an accordion-like structure.

Longitudinal sections of the ephyra-detachment-phase strobilae showed that the tips of the invaginations were fused (Fig. 2e, j) and the gastric cavity was divided. Consequently, each segment (ephyra) had a closed gastric cavity.

BrdU labeling in polyps/strobilae

To detect cell proliferation during strobilation, BrdU labeling experiments were performed on polyps and strobilae at various stages. BrdU, an analog of thymidine, can be incorporated into the newly synthesized DNA of proliferating cells during the S phase of the cell cycle. Cells that proliferated during incubation with BrdU were visualized using an anti-BrdU antibody (Gratzner et al. 1975). As shown in Fig. 3, the polyps are labeled by incubation with BrdU for 48 h at 23 ºC. Prestrobilae, segmentation-phase strobilae, and ephyra-morphogenesis-phase strobilae were prepared by CS treatment, and then labeled by incubation with BrdU for 24 h at 23 ºC.

Polyp.

The polyps did not exhibit budding during incubation with BrdU. Furthermore, only a few signals were detected in the body columns of the longitudinal sections (Fig. 4a).

Prestrobila.

During incubation with BrdU, prestrobilae did not show any morphological changes. On the

longitudinal sections of BrdU-labeled prestrobilae, signals were observed beneath the tentacles where the first segment would be generated (Fig. 4b; dotted brackets), but not in the aboral half of the body column, including the foot region.

Segmentation-phase strobila.

During incubation with BrdU, an additional 2–3 segments were generated (Fig. 4c; solid brackets). In longitudinal sections of BrdU-labeled strobilae, signals were observed in segments that had been generated before incubation (Fig. 4c; dashed brackets) and segments that were generated during incubation (Fig. 4c; solid brackets). Moreover, the region beneath the most aboral constriction, where the next segment should be newly generated, also exhibited signals (Fig. 4c; dotted brackets). However, only a few signals were detected in the foot region.

Ephyra-morphogenesis-phase strobila.

Ephyra morphogenesis progressed from the early to middle ephyra morphogenesis phases during incubation with BrdU. Signals were observed in all segments of the longitudinal sections of BrdU-labeled strobilae (Fig. 4d).

In the prestrobilae and strobilae, cell proliferation was observed in the endodermal and ectodermal epithelial cell layers (Fig. 4e–g).

Effect of a cell cycle inhibitor on strobilation

To examine the involvement of cell proliferation in strobilation, HU, an inhibitor of the cell cycle (Sinclair 1965), was administered to the polyps/strobilae at each stage of strobilation. Strobilation was induced by MMI and HU was administered at 0 (experiment A), 24 (experiment B), 48 (experiment C), or 72 h (experiment D) after the administration of MMI, according to the administration schedule shown in Fig. 5.

In the control group, in which HU was not administered, the first constriction appeared beneath the tentacles 24–48 h after MMI administration (onset of strobilation). Subsequently, additional segments were sequentially generated from the oral side to the aboral side (segmentation phase). The tentacles around

the mouth were degenerating 72 h after MMI administration (early ephyra morphogenesis phase). Thereafter, each segment developed into an ephyra (middle ephyra morphogenesis phase), and 6–15 ephyrae were released from each polyp at 10 days (ephyra detachment phase).

In experiment A, HU was co-administered to polyps with MMI. Strobilation did not start within 10 days; the number of segments was zero ($p < 0.01$ vs control, Mann–Whitney *U* test with Bonferroni correction) (Fig. 6a; Exp. A). All animals remained polyps without any morphological abnormalities on the 10th day.

In experiment B, HU was administered to the prestrobilae. No constrictions were generated within 10 days; the number of segments was zero ($p < 0.01$ vs control) (Fig. 6a; Exp. B).

In experiment C, HU was administered to the segmentation-phase strobilae, in which the number of segments was 2–4. The number of segments generated in 10 days was significantly smaller than that in the control group ($p < 0.05$ vs control) (Fig. 6a; Exp. C). The increase in number of segments (Δsegment) was also significantly smaller than that in the control group ($p < 0.01$ vs control) (Fig. 6b). All animals in this group showed abnormal morphologies, in that the body column was partially bulging (Fig. 7a). Histological observations revealed that the mesoglea, an area between the endodermal and ectodermal epithelial cell layers, was thickened in abnormal strobilae (Fig. 7b) compared to normal segmentation-phase strobilae (Fig. 2c, h). None of the tested animals shifted to the ephyra morphogenesis phase.

In experiment D, HU was administered to the early ephyra morphogenesis phase. The number of segments showed no significant difference compared to that in the control group (Fig. 6a; Exp. D). Although all tested animals shifted to the middle ephyra morphogenesis phase, the morphology of the segments metamorphosing into ephyrae was impaired (Fig. 7c). Ephyrae released from these abnormal strobilae showed an aberrant morphology in that they appeared to be bulging (Fig. 7d) and smaller than the normal ephyrae (Fig. 7g). HE-stained sections showed that the mesoglea was thickened in the abnormal ephyrae (Fig. 7e, f) compared to that in the normal ephyrae (Fig. 7h, i), resembling the bulging strobilae observed in experiment C (Fig. 7b).

Discussion

Morphological change during strobilation

Prior to histological analyses of BrdU-labeled or HU-treated polyps/strobilae, the internal

morphology was observed by HE staining of paraffin-embedded sections. Here, sac-like structures, which is composed of ectodermal and endodermal epithelial cell layers, formed the gastric cavity in both the polyps (Fig. 2a, f) and the prestrobilae (Fig. 2b, g). No morphological differences between the polyps and prestrobilae were observed.

In the segmentation phase, both epithelial cell layers invaginated into the gastric cavity at regular intervals sequentially from the oral side to the aboral side (Fig. 2c, h). The tips of the invaginated epithelial layers were also unfused at the constrictions, indicating that the segmentation-phase strobilae possessed an accordion-like structure topologically equivalent to the sac-like structure of polyps and strobilae.

In the ephyra morphogenesis phase, the two epithelial cell layers invaginated deeper than in the segmentation phase; the tips of the invaginations were unfused at the middle ephyra morphogenesis phase (Fig. 2d, i). The middle ephyra-morphogenesis-phase strobilae also maintained an accordion-like structure characterized by undivided gastric cavities, even during the formation of the ephyra morphology.

In the ephyra detachment phase, the tips of the invaginations were fused (Fig. 2e, j), suggesting that the gastric cavity was likely to be divided during the late ephyra morphogenesis phase and ephyra detachment phase.

Hence, the strobilation process in the internal morphology can be summarized as follows: (i) first constriction is induced at the initiation of strobilation, in which the endodermal and ectodermal epithelial cell layers beneath the tentacles invaginated into the gastric cavity; (ii) second constriction is then induced when cell layers invaginated beneath the first constriction; (iii) multiple segments are produced sequentially from the oral to aboral sides when invaginations occur repeatedly at regular intervals; (iv) each segment develops an ephyra morphology, during which it maintains an undivided gastric cavity; and (v) ephyrae were sequentially detached from the oral side to the aboral side after the tips of the invaginations were fused.

Cell proliferation during strobilation

In the present study, to examine stage-associated roles of cell proliferation on strobilation of *A. coerulea*, BrdU labeling experiments were performed to visualize cell proliferation in polyps/strobilae at various stages. In addition, the cell cycle inhibitor HU was administered to the polyps/strobilae at each stage. The histochemical and pharmacological results suggest that cell proliferation plays a distinct role in every stage of strobilation (initiation of strobilation, segmentation, and ephyra morphogenesis), except in

ephyra detachment.

Initiation of strobilation.

In BrdU labeling experiments, cell proliferation was observed in the area beneath the tentacles of the prestrobilae, which is the prospective region of the first segment (Fig. 4b). When HU was administered before the onset of strobilation, strobilation did not begin (Fig. 6a; Exp. A, B). These results suggest that cell proliferation in the prospective region of the first segment is essential for the initiation of strobilation. Our two previous studies revealed that the first segment, defined as the area between the oral end and the first constriction, can drive subsequent segmentation and ephyra morphogenesis. First, strobilation induced by decreasing the water temperature proceeds to the end, even at room temperature, after the first segment is generated (Misaki et al. 2023). Second, indomethacin-induced strobilation was completed in the absence of indomethacin after generation of the first segment (Kuniyoshi et al. 2012). Thus, the formation of the first segment was sufficient to continue strobilation. Collectively, our findings suggest that cell proliferation may contribute to the initiation of strobilation by preparing the first segment.

In contrast to prestrobilae (Fig. 4b), signals were not detectable in the body columns of polyps incubated with BrdU (Fig. 4a). It has been reported that cell proliferation is observed in the budding regions (Balcer and Black 1991) and tentacles of polyps (Gold et al. 2015). However, there were very few labeled cells in the polyps in this study, probably because of starvation before BrdU treatment. Under starvation conditions, budding was not observed during incubation, and the exhaustion of tentacles and their nematocysts could be very low without feeding behavior. Therefore, cell proliferation may occur infrequently in starved polyps.

Although there were no morphological differences between the polyps and the prestrobilae (Fig. 2a, b), prestrobilae are considered physiologically different from the polyps in that cell proliferation occurred beneath the tentacles in the prestrobilae but not in the polyps.

Segmentation.

In BrdU labeling, cell proliferation was observed intensively in already-formed segments and in the prospective region of the next segment (Fig. 4c). When HU was administered during the segmentation phase, the generation of new segments ceased after one to three segments had been generated (Fig. 6b), suggesting a lag time between the administration of HU and the inhibition of cell proliferation. Nevertheless, the number of segments generated in HU-treated strobilae was lower than that in normal strobilae (Fig. 6a, b), suggesting that cell proliferation was required for segmentation.

The ectodermal and endodermal epithelial cell layers were repetitively invaginated to produce segments (Fig. 2c, h). Cell proliferation was observed in both layers of segments in an interspersed pattern (Fig. 4c, f), suggesting that the number of cells in the segments should increase during segmentation. Strobilae treated with HU during the segmentation phase exhibited abnormally bulged body columns (Fig. 7a). Histological observations revealed that these bulges likely resulted from the thickening of the mesoglea (Fig. 7b). Because inhibition of cell proliferation causes a shortage of cells to expand the epithelial layers and the mesogleal space, the volume of the mesoglea could be insufficient to retain extracellular matrix proteins. Therefore, a significant amount of extracellular matrix proteins may accumulate in a small volume of the mesoglea, resulting in thickened mesoglea in HU-treated strobilae.

Notably, cell proliferation was observed in the prospective region of the next segment (Fig. 4c; dotted brackets). This indicated that cell proliferation started prior to invagination of the epithelial layers. The inhibitory effect of HU on segment generation (Fig. 6b) may have resulted from the interruption of cell proliferation in the prospective region of the next segment.

Ephyra morphogenesis.

BrdU labeling experiments revealed that cell proliferation in the segments occurred continuously during the ephyra morphogenesis phase (Fig. 4d). Interestingly, in the segmentation-phase strobilae, cell proliferation was detected in the segments which had been generated before BrdU incubation (Fig. 4c; dashed brackets). Thus, it is possible that the cell proliferation necessary for ephyra morphogenesis begins immediately after segment generation. Administration of HU disturbed ephyra morphogenesis (Fig. 7c). Ephyrae released from the HU-treated strobilae showed an abnormal morphology (Fig. 7d) and were smaller than the normal ephyrae (Fig. 7g). The decrease in cell number caused by the inhibition of cell proliferation can lead to a small body size. Furthermore, these aberrant ephyrae were bulging (Fig. 7d) and had thickened mesoglea (Fig. 7e, f), similar to the defects of HU-treated, segmentation-phase strobilae (Fig. 7a, b). As in the case of strobilae, aberrant ephyrae may lack mesogleal space to retain extracellular matrix proteins. Thus, cell proliferation is required to develop the ephyra morphology.

Ephyra detachment.

When HU was administered during the ephyra morphogenesis phase, abnormal ephyrae were detached (Fig. 7c, d). Although ephyra morphogenesis was defective, HU did not disturb ephyra release, suggesting that cell proliferation may not be necessary for ephyra detachment.

The next question is “What molecules induce cell proliferation during strobilation?” One such candidate is the Wnt family of proteins. In *Hydra* species, the Wnt-3 protein induced cell proliferation in response to apoptosis during head regeneration (Chera et al. 2009). Recent genome projects (Gold et al. 2019; Khalturin et al. 2019) also revealed that all members of the *Wnt* gene family, except for *Wnt-9* and *Wnt-10*, are present in the *Aurelia* genome. In transcriptome analysis, some *Wnt* genes showed stage-specific expression during strobilation; for example, *Wnt-16b* was upregulated in segmentation-phase strobilae (Brekhman et al. 2015). Although further studies are required to identify the factors that induce cell proliferation during strobilation, secretory proteins are potential candidates.

In summary, we demonstrated that cell proliferation is required for the initiation of strobilation, segmentation, and ephyra morphogenesis during strobilation of *A. coerulea*. During the initiation of strobilation, cell proliferation may play an important role in generating the first segment, which drives subsequent strobilation steps. During segmentation, cell proliferation occurred in the prospective region of the next segment prior to invagination of the epithelial layers, suggesting that cell proliferation might have participated in the generation of a new segment. In ephyra morphogenesis, cell proliferation is crucial for the normal morphology and body size of the ephyrae, but it is not necessary for ephyra detachment.

Acknowledgements

We would like to express our gratitude to M. Shimada and T. Kawai of Graduate School of Integrated Science for Life, Hiroshima University for their kind advice concerning histological experiments and permission to use microtome. We greatly thank S. Ohtsuka and S. Iwasaki of the Takehara Marine Science Station of Hiroshima University for providing the filtered seawater. We would like to thank Editage (www.editage.com) for English language editing. We wish to thank the reviewers for carefully reading and giving helpful comments on this manuscript.

Funding

Japan Society for the Promotion of Science (JSPS) KAKENHI, Grant number 16K14916, 19KK0149, and 20K05851.

Declarations

Conflict of interest None.

References

Balcer LJ, Black RE (1991) Budding and strobilation in Aurelia (Scyphozoa, Cnidaria): functional requirement and spatial patterns of nucleic acid synthesis. Roux's Arch Dev Biol 200:45–50. doi: 10.1007/BF02457640

Brekhman V, Malik A, Haas B, Sher N, Lotan T (2015) Transcriptome profiling of the dynamic life cycle of the scypohozoan jellyfish Aurelia aurita. BMC Genomics 16–74. doi: 10.1186/s12864-015-1320-z

Chera S, Ghila L, Dobretz K, Wenger Y, Bauer C, Buzgariu W, Martinou JC, Galliot B (2009) Apoptotic cells provide an unexpected source of Wnt3 signaling to drive hydra head regeneration. Dev Cell 17:279–289. doi: 10.1016/j.devcel.2009.07.014

Collins AG, Schuchert P, Marques AC, Jankowski T, Medina M, Schierwater B (2006) Medusozoan phylogeny and character evolution clarified by new large and small subunit rDNA data and an assessment of the utility of phylogenetic mixture models. Syst Biol 55(1):97–115. doi: 10.1080/10635150500433615

Dawson MN, Jacobs DK (2001) Molecular evidence for cryptic species of Aurelia aurita (Cnidaria, Scyphozoa). Biol Bull 200:92–96

Fuchs B, Wang W, Graspeuntner S, Li Y, Insua S, Herbst EM, Dirksen P, Bohm AM, Hemmrich G, Sommer F, Domazet-Loso T, Klostermeier UC, Anton-Erxleben F, Rosenstiel P, Bosch TCG, Khalturin K (2014) Regulation of polyp-to-jellyfish transition in Aurelia aurita. Curr Biol 24:263–273. doi: 10.1016/j.cub.2013.12.003

Fujita S, Kuranaga E, Nakajima Y (2019) Cell proliferation controls body size growth, tentacle morphogenesis, and regeneration in hydrozoan jellyfish Cladonema pacificum. PeerJ 7:e7579. doi: 10.7717/peerj.757

Gold DA, Katsuki T, Li Y, Yan X, Regulski M, Ibberson D, Holstein T, Steele RE, Jacobs DK, Greenspan RJ (2019) The genome of the jellyfish Aurelia and the evolution of animal complexity. Nat Ecol Evol 3:96–104. doi: 10.1038/s41559-018-0719-8

Gold DA, Nakanishi N, Hensley NM, Cozzolino K, Tabatabaee M, Martin M, Hartenstein V, Jacobs DK (2015) Structure and developmental disparity in the tentacles of the moon jellyfish Aurelia sp.1. PLoS ONE 10(8):e0134741. doi: 10.1371/journal.pone.0134741

Gold DA, Nakanishi N, Hensley NM, Hartenstein V, Jacobs DK (2016) Cell tracking supports secondary gastrulation in the moon jellyfish Aurelia. Dev Genes Evol 226:383–387. doi: 10.1007/s00427-016-0559-y

Gratzner HG, Leif RC, Ingram DJ, Castro A (1975) The use of antibody specific for bromodeoxyuridine for the immunofluorescent determination of DNA replication in single cells and chromosomes. Exp Cell Res 95:88–94

Gurska D, Garm A (2014) Cell proliferation in cubozoan jellyfish Tripedalia cystophora and Alatina moseri. PLoS One 9(7):e102628. doi: 10.1371/journal.pone.0102628

Helm RR, Dunn CW (2017) Indoles induce metamorphosis in a broad diversity of jellyfish, but not in a crown jelly (Coronatae). PLoS One 12(12):e0188601. doi: 10.1371/journal.pone.0188601

Ishizuya-Oka A, Ueda S (1996) Apoptosis and cell proliferation in the Xenopus small intestine during metamorphosis. Cell Tissue Res 286:467–476. doi: 10.1007/s004410050716

Khalturin K, Shinzato C, Khalturina M, Hamada M, Fujie M, Koyanagi R, Kanda M, Goto H, Anton-Erxleben F, Toyokawa M, Toshino S, Satoh N (2019) Medusozoan genomes inform the evolution of the jellyfish body plan. Nat Ecol Evol 3:811–822

Kraus JEM, Fredman D, Wang W, Khalturin K, Technau U (2015) Adoption of conserved developmental genes in development and origin of the medusa body plan. EvoDevo 6:23. doi: 10.1186/s13227-015-0017-3

Kroiher M, Siefker B, Berking S (2000) Induction of segmentation in polyps of Aurelia aurita (Scyphozoa, Cnidaria) into medusae and formation of mirror-image medusa anlagen. Int J Dev Biol 44:485–490

Kuniyoshi H, Okumura I, Kuroda R, Tsujita N, Arakawa K, Shoji J, Saito T, Osada H (2012) Indomethacin induction of metamorphosis from the asexual stage to sexual stage in the moon jellyfish Aurelia aurita. Biosci Biotechnol Biochem 76(7):1397–1400. doi: 10.1271/bbb.120076

Milán M, Campuzano S, García-Bellido A (1996) Cell cycling and patterned cell proliferation in the Drosophila wing during metamorphosis. Proc Natl Acad Sci 93:11687–11692. doi: 10.1073/pnas.93.21.11687

Misaki Y, Hirashima T, Fujii K, Hirata A, Hoshino Y, Sumiyoshi M, Masaki S, Suzuki T, Inada K, Koyama H, Kuniyoshi H, Arakawa K (2023) 4-Methoxy-2,2'-bipyrrole-5-carbaldehyde, a biosynthetic intermediate of bipyrrolecontaining natural products from the Streptomyces culture,arrests the strobilation of moon jellyfish Aurelia coerulea. Front Mar Sci doi: 10.3389/fmars.2023.1198136

Plickert G, Kroiher M, Munck A (1988) Cell proliferation and early differentiation during embryonic development and metamorphosis of Hydractinia echinata. Development 103:795–803

Scorrano S, Aglieri G, Boero F, Dawson MN, Piraino S (2016) Unmasking Aurelia species in the

Mediterranean Sea: an integrative morphometric and molecular approach. Zool J Linn Soc. doi: 10.1111/zoj.12494

Sinclair WK (1965) Hydroxyurea: differential lethal effects on cultured mammalian cells during the cell cycle. Science 150(3704):1729–1731. doi: 10.1126/science.150.3704.1729

Tsujita N, Kuwahara H, Koyama H, Yanaka N, Arakawa K, Kuniyoshi H (2017) Molecular characterization of aspartylglucosaminidase a lysosomal hydrolase upregulated during strobilation in the moon jellyfish Aurelia aurita. Biosci Biotechnol Biochem 81(5):938–950. doi: 10.1080/09168451.2017.1285686

Figure legends

Fig. 1 Strobilation of *A. coerulea* induced by cold shock

(a) Polyp. (b) Prestrobila, an animal prior to segmentation. (c) Segmentation-phase strobila with a single constriction. (d) Segmentation-phase strobila with five segments. (e) Segmentation-phase strobila with seven segments. (f) Early ephyra-morphogenesis-phase strobila during degeneration of tentacles. (g) Middle ephyra-morphogenesis-phase strobila after degeneration of tentacles. (h) Late ephyra-morphogenesis-phase strobila with pulsating ephyrae. (i) Ephyra-detachment-phase strobila with three ephyrae, which had already released seven ephyrae. (j) Liberated ephyra. (k) Residuum after detachment of all ephyrae. Scale bar: 1 mm.

Fig. 2 Hematoxylin-eosin stain of strobilae induced by cold shock

Longitudinal sections of the (a) polyp, (b) prestrobila, (c) segmentation-phase strobila with eight segments, (d) middle ephyra-morphogenesis-phase strobila with nine segments, and (e) ephyra-detachment-phase strobila with two ephyrae. High-magnification views of the boxed areas in (a–e) are shown in (f–j). Oral is at the top (a–e). White double-headed arrows indicate the ectodermal and endodermal epithelial cell layers. The black arrowheads indicate constriction. The white arrowhead in (j) indicates fusion of the invagination tips. tn: tentacles, gc: gastric cavity, m: mouth, ft: foot, ec: ectoderm, en: endoderm, mes: mesoglea. Scale bar: 100 µm (a–e) and 20 µm (f–j).

Fig. 3 Incubation schedule of BrdU labeling experiment

Polyps were collected from a Petri dish that was cultured at 23 ºC (unfilled bar) and incubated in FSW containing 10 mM BrdU for 48 h at 23 ºC (hatched bar), followed by fixation with 4% formaldehyde in ASW (solid triangle). Strobilation was induced by CS. Prestrobilae, segmentation-phase strobilae, and ephyra-morphogenesis-phase strobilae were collected from Petri dishes cultured at 10 ºC (filled bars). Collected strobilae were incubated in FSW containing 10 mM BrdU for 24 h at 23 ºC (hatched bars), followed by fixation with 4% formaldehyde in ASW (solid triangles). Illustrations above the hatched bars indicate the morphology of animals at the time of BrdU administration (left) and fixation (right). The numbers in parentheses represent sample sizes.

Fig. 4 Immunostained sections of BrdU-labeled polyps and strobilae

Longitudinal sections of BrdU-labeled (a) polyps, (b) prestrobilae, (c) segmentation-phase strobilae, and (d) middle ephyra-morphogenesis-phase strobilae stained with anti-BrdU and alkaline phosphatase-conjugated secondary antibodies. High-magnification views of the boxed areas in (b–d) are shown in (e–g). Dashed brackets indicate segments that had been generated prior to BrdU incubation. Solid brackets indicate the segments generated during BrdU incubation. Dotted brackets indicate the prospective regions of the next segment. The nuclei of the proliferating cells were detected as purple spots. White double-headed arrows indicate the ectodermal and endodermal epithelial cell layers. Black arrows in (e) show the detected nuclei. Spots in the tentacles should be nonspecific signals of the secondary antibody since they were detected in the negative control staining without the anti-BrdU antibody. Oral is at the top. tn: tentacles, m: mouth, ft: foot, ec: ectoderm, en: endoderm. Scale bar: 100 μm (a–d) and 20 μm (e–g).

Fig. 5 Administration schedule of the cell cycle inhibitor, hydroxyurea (HU)

Strobilation was induced by administration of MMI. The time-course characteristics of MMI-induced strobilation are shown in the illustration of top panel: (left to right) polyp (0 h), prestrobila (24 h), segmentation-phase strobila with a single constriction, segmentation-phase strobila with 2–4 segments (48 h), early ephyra-morphogenesis-phase strobila (72 h), middle ephyra-morphogenesis-phase strobila (120 h), ephyra-detachment-phase strobila (144 h), and completion of the ephyra release (240 h). Black horizontal arrows indicate the incubation with MMI. Gray horizontal arrows indicate the incubation with HU. In experiment A (Exp. A), HU was co-administered with MMI to the polyps. In experiment B (Exp. B), HU was administered to the prestrobilae 24 h after MMI administration. In experiment C (Exp. C), HU was administered to the segmentation-phase strobilae 48 h after MMI administration. In experiment D (Exp. D), HU was administered to the early ephyra morphogenesis phase 72 h after MMI administration. In the control (Cont.), HU was not added.

Fig. 6 Effect of HU on segmentation

MMI and HU were administered according to the schedule shown in Fig. 5. HU was added at 0 (Exp. A), 24 (Exp. B), 48 (Exp. C), or 72 h (Exp. D) after MMI administration. In the control (Cont.), HU was not

added. (a) Number of segments 10 days after MMI administration. (b) The increase in number of segments (Δsegment) following HU administration in Exp. C. The numbers in parentheses represent sample sizes. * $p < 0.05$, ** $p < 0.01$ vs control, Mann–Whitney *U* test with Bonferroni correction.

Fig. 7. Abnormal morphology caused by HU

(a) A typical example of abnormal morphology observed in experiment C. A part of the body column was bulging (white arrow). (b) HE-stained longitudinal section of the abnormal strobila shown in (a). The mesoglea of the strobila was thickened. (c) A typical example of abnormal morphology observed in experiment D. The strobila shifted from the early ephyra morphogenesis phase to the middle ephyra morphogenesis phase; however, segments metamorphosing into ephyrae were defective. (d) An abnormal ephyra liberated from the strobila shown in (c). (e) HE-stained section of the abnormal ephyra. The mesoglea of the ephyra was thickened, similar to the defect observed in (b). (g) Normal ephyra induced by MMI. (h) HE-stained section of normal ephyra. High-magnification views of the boxed areas in (e, h) are shown in (f, i). Oral is at the top (a–c). Arrowheads indicate constrictions. gc: gastric cavity, m: mouth, ft: foot, ec: ectoderm, en: endoderm, mes: mesoglea. Scale bar: 1 mm (a, c, d, g), 100 μm (b, e, f, h, i).

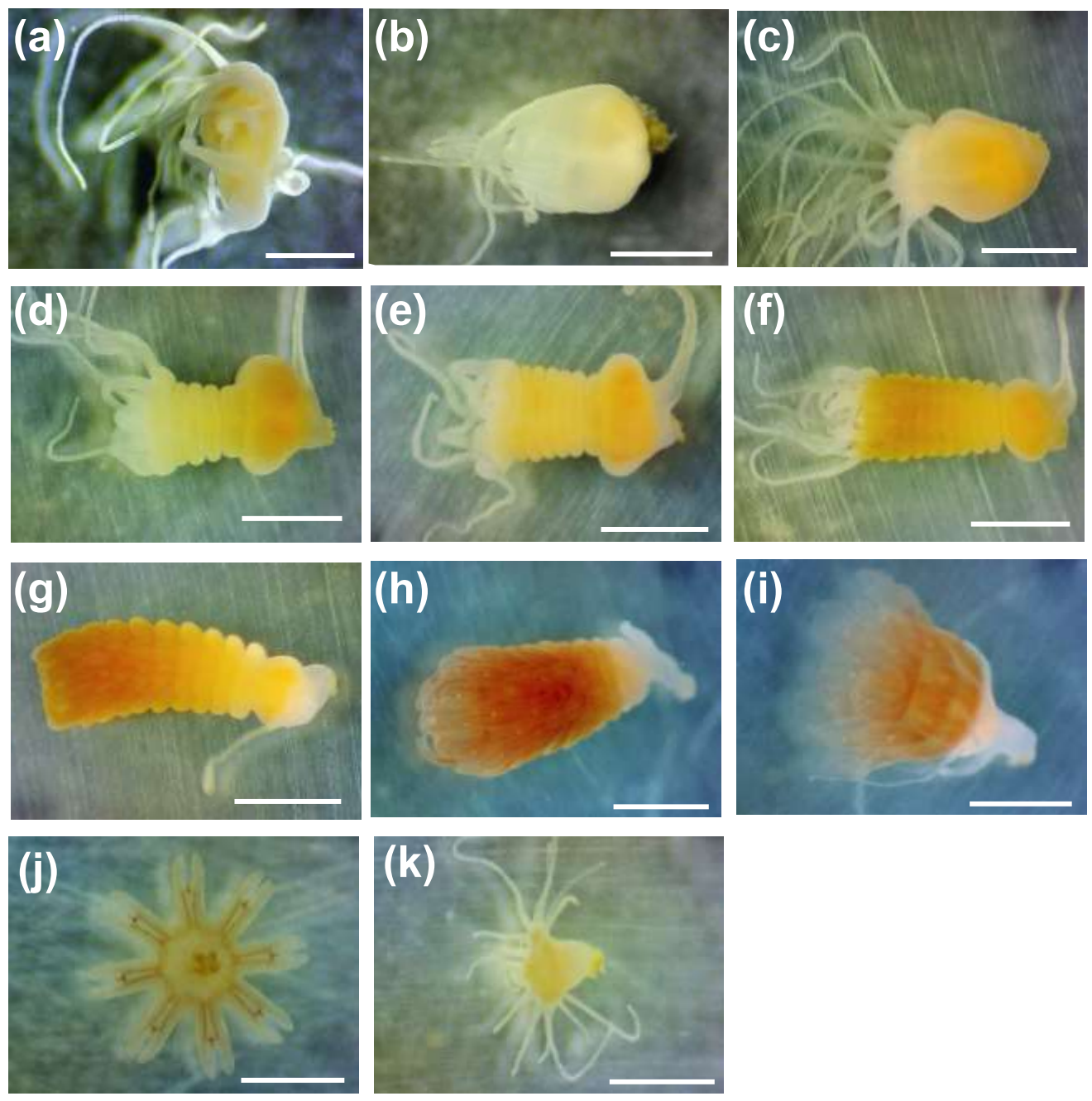

Fig. 1 Strobilation of *A. coerulea* induced by cold shock

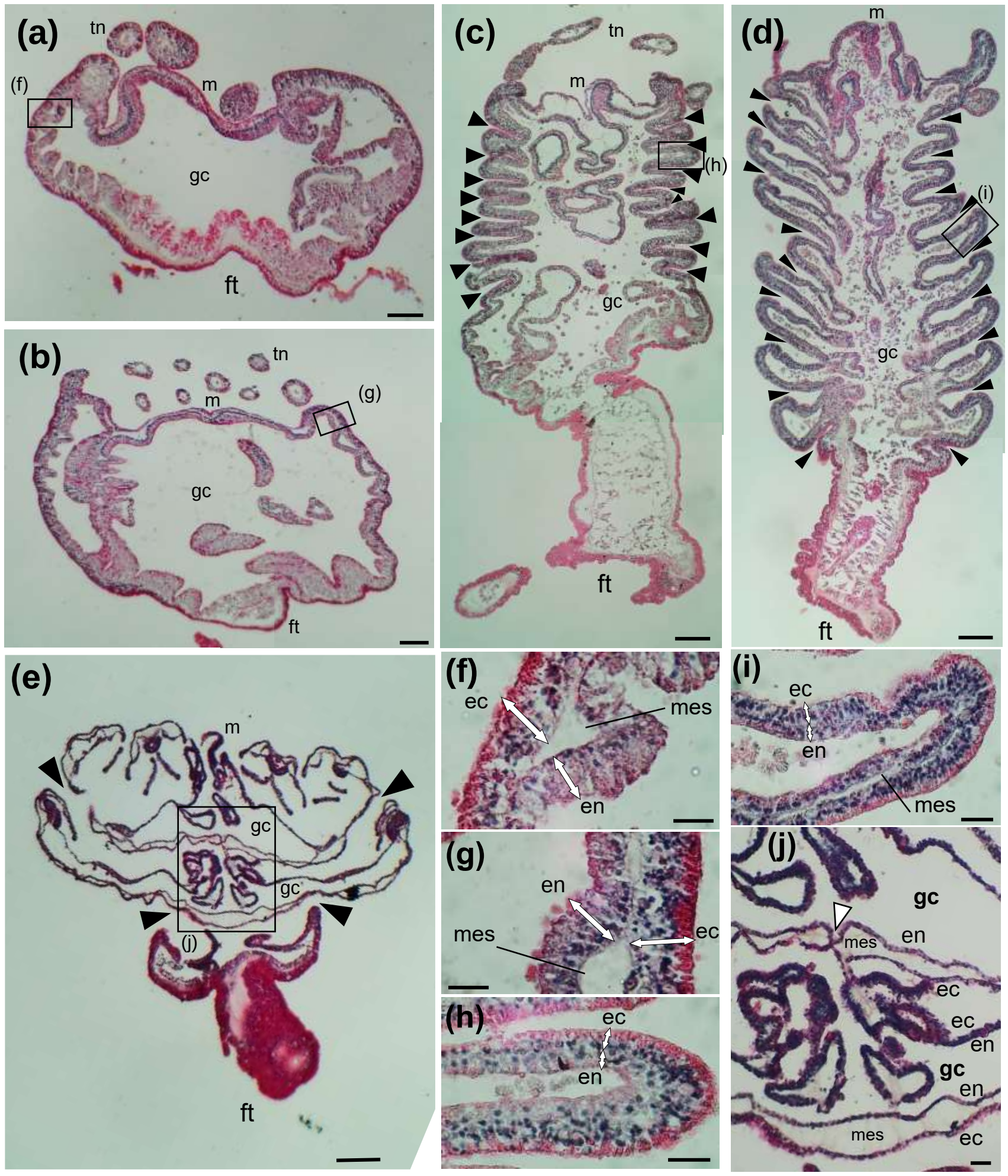

Fig. 2 Hematoxylin-eosin stain of strobilae induced by cold shock

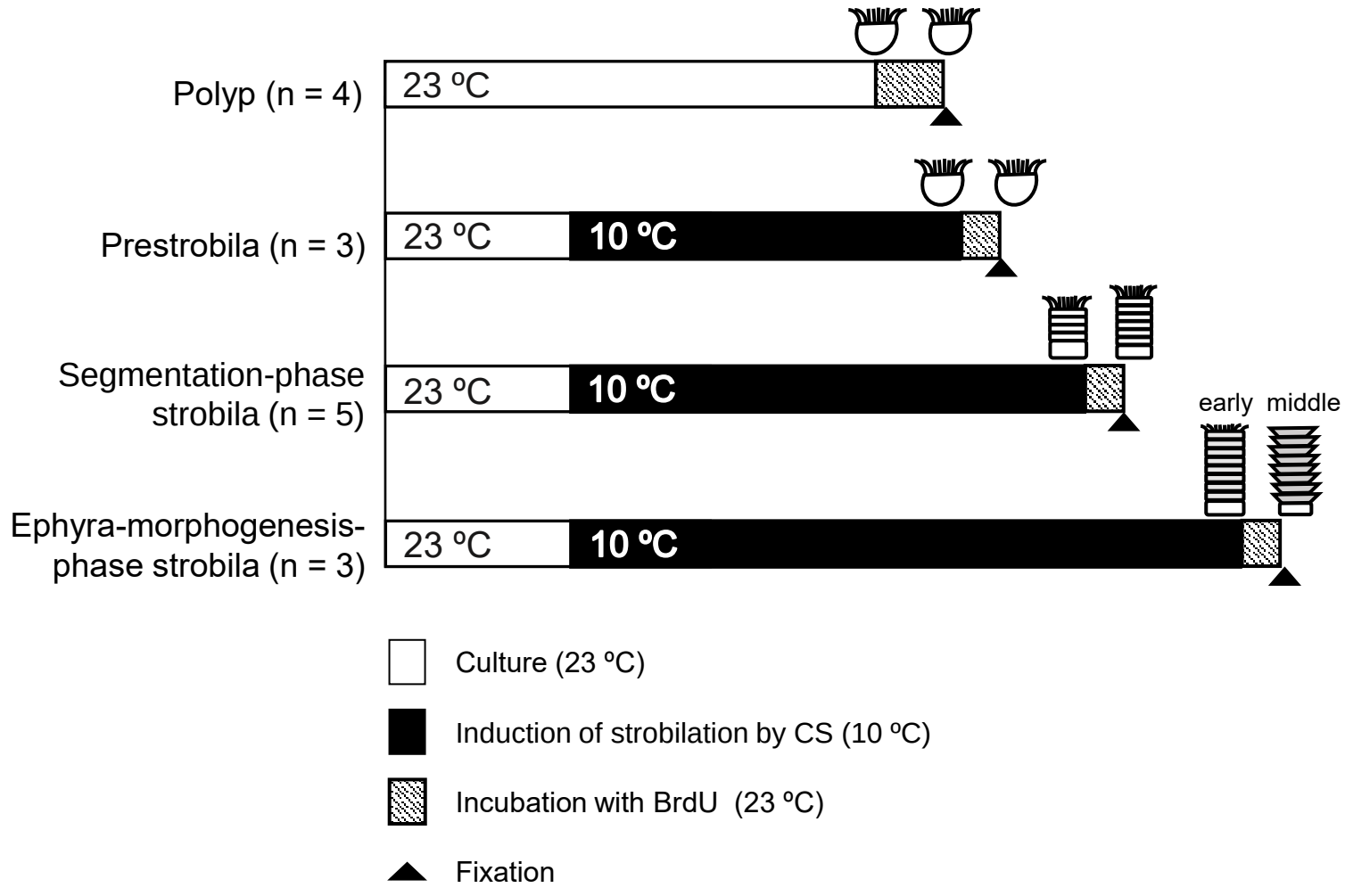

Fig. 3 Incubation schedule of BrdU labeling experiment

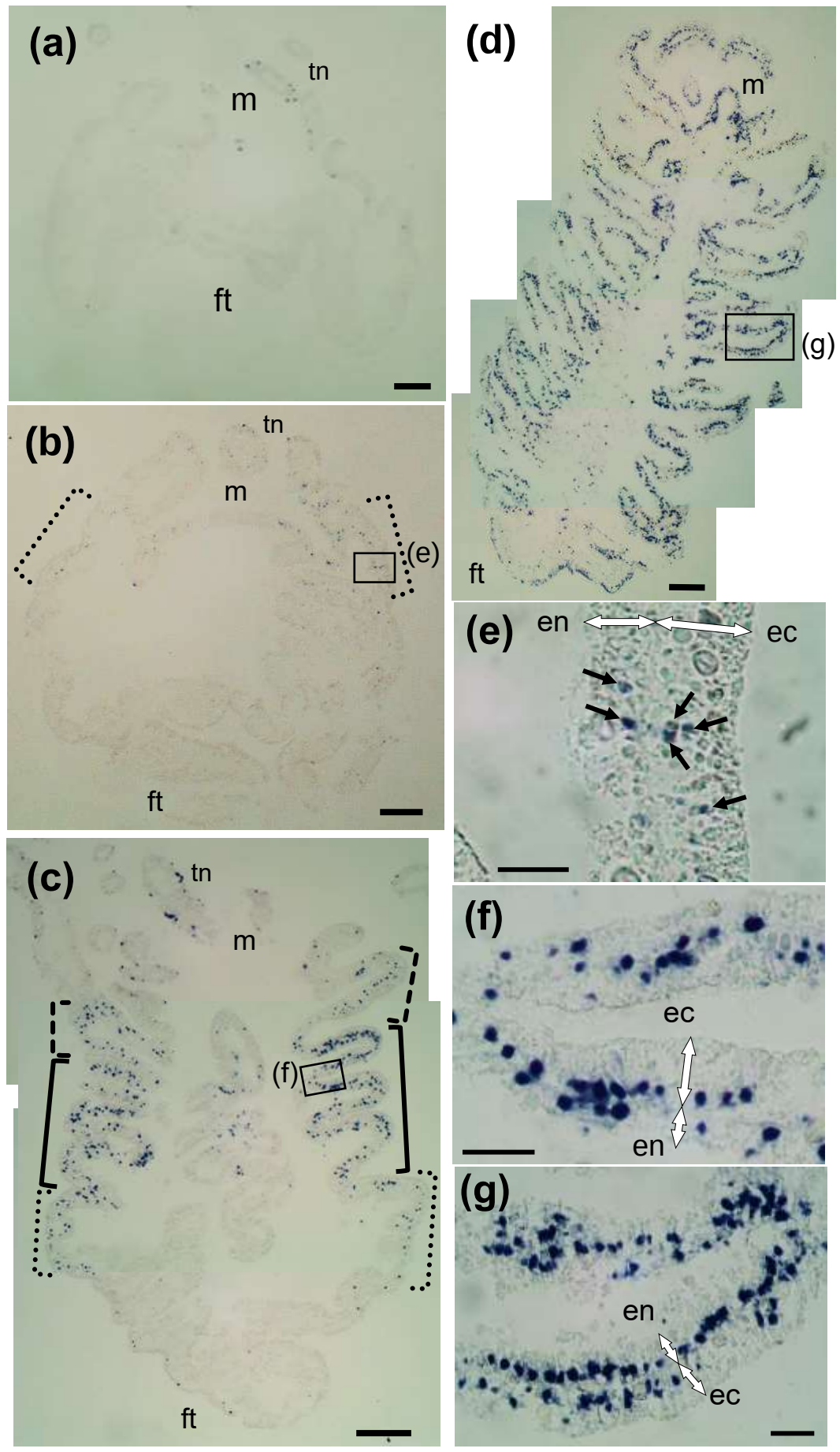

Fig. 4 Immunostained sections of BrdU-labeled polyps and strobilae

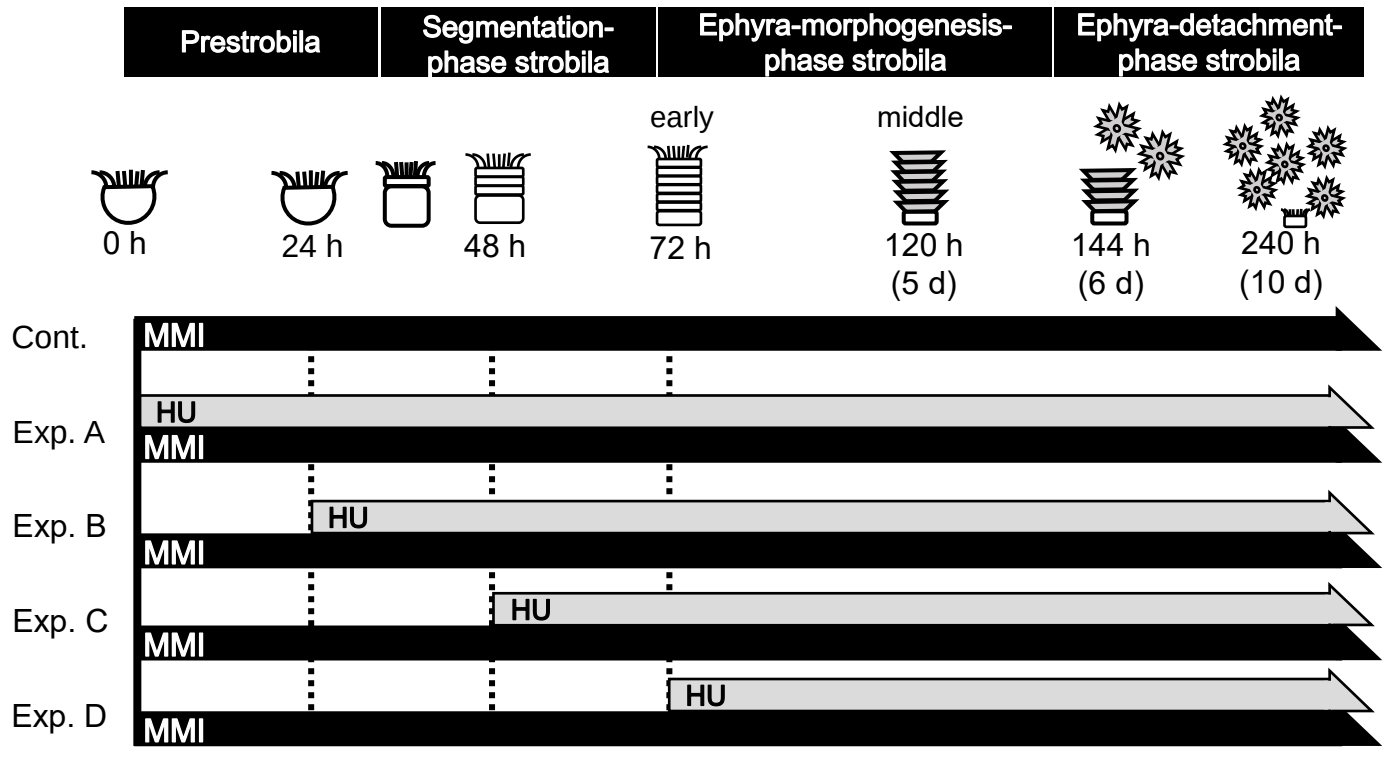

Fig. 5 Administration schedule of the cell cycle inhibitor, hydroxyurea (HU)

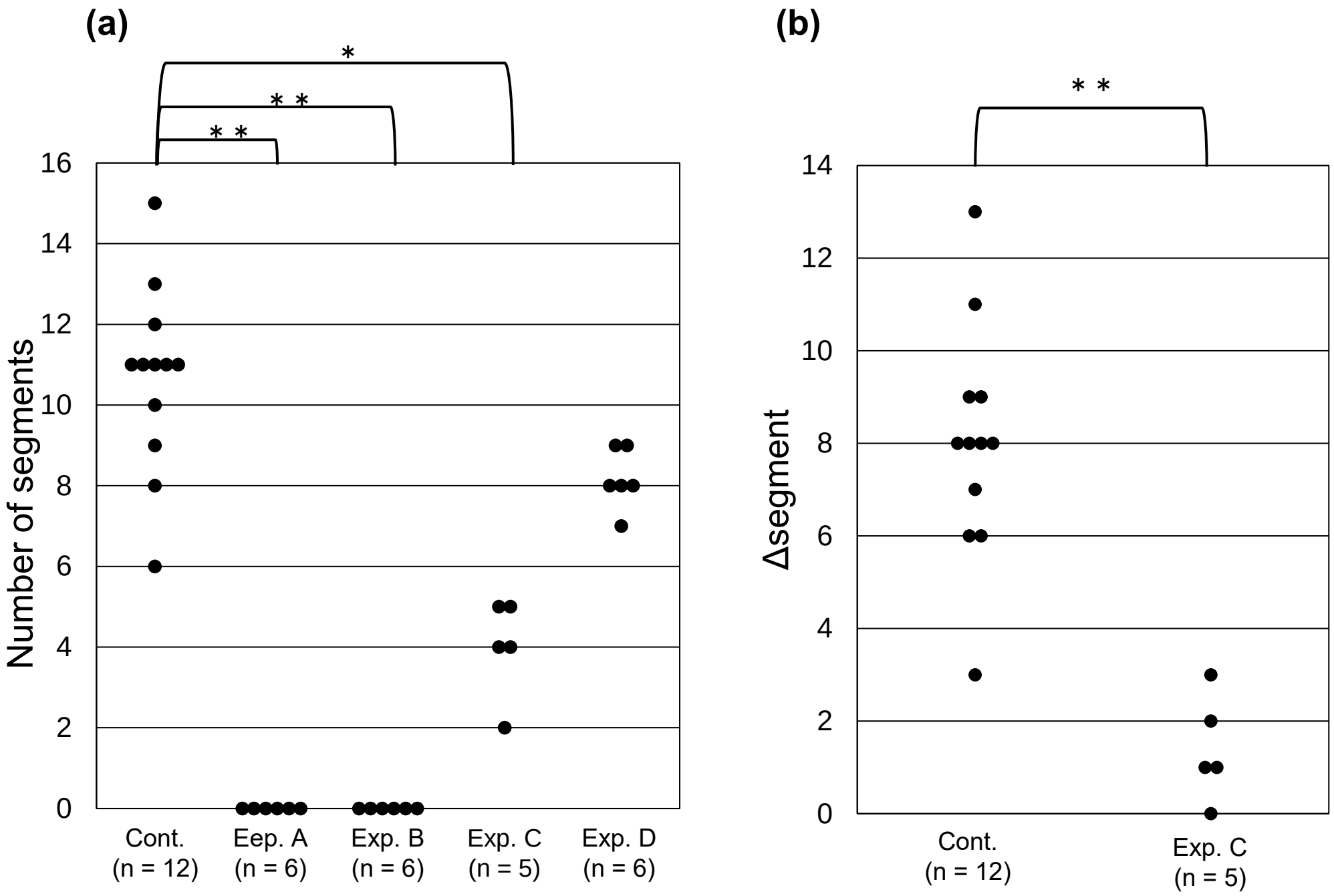

Fig. 6 Effect of HU on segmentation

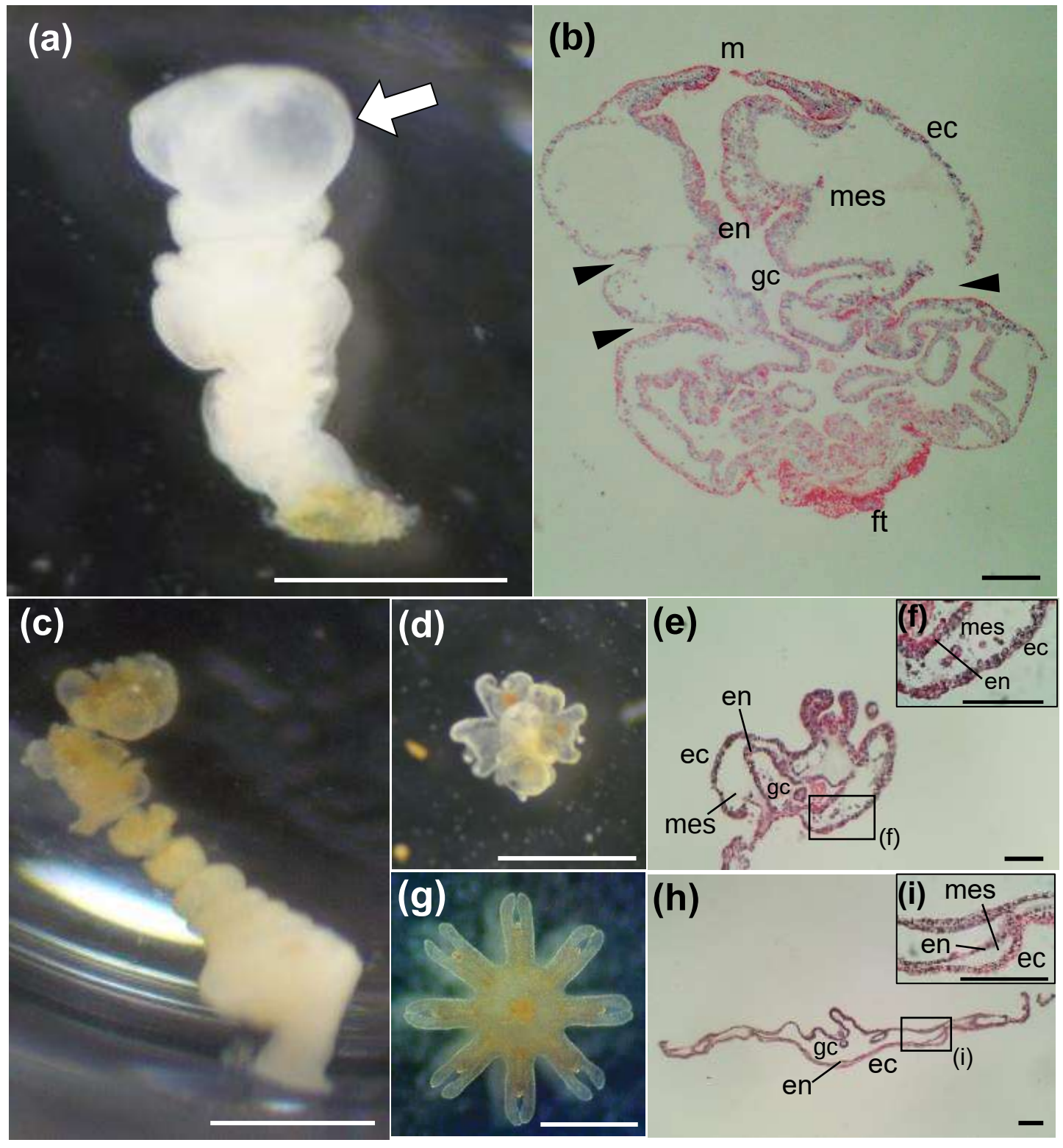

Fig. 7. Abnormal morphology caused by HU